

# (Global and local) fluctuations of phase space contraction in deterministic stationary nonequilibrium

F. Bonetto<sup>a)</sup>

*Department of Mathematics, Rutgers University, New Brunswick, New Jersey 08903*

N. I. Chernov

*Department of Mathematics, University of Alabama in Birmingham, Birmingham, Alabama 35249*

J. L. Lebowitz

*Department of Mathematics and Physics, Rutgers University, New Brunswick, New Jersey 08903*

(Received 16 April 1998; accepted for publication 17 June 1998)

We studied numerically the validity of the fluctuation relation introduced in Evans *et al.* [Phys. Rev. Lett. **71**, 2401–2404 (1993)] and proved under suitable conditions by Gallavotti and Cohen [J. Stat. Phys. **80**, 931–970 (1995)] for a two-dimensional system of particles maintained in a steady shear flow by Maxwell demon boundary conditions [Chernov and Lebowitz, J. Stat. Phys. **86**, 953–990 (1997)]. The theorem was found to hold if one considers the total phase space contraction  $\sigma$  occurring at collisions with both walls:  $\sigma = \sigma^\uparrow + \sigma^\downarrow$ . An attempt to extend it to more local quantities  $\sigma^\uparrow$  and  $\sigma^\downarrow$ , corresponding to the collisions with the top or bottom wall only, gave negative results. The time decay of the correlations in  $\sigma^{\uparrow,\downarrow}$  was very slow compared to that of  $\sigma$ . © 1998 American Institute of Physics. [S1054-1500(98)00104-9]

**While fluctuations in the total phase space volume contraction of a realistically thermostatted computer model system with shear flow satisfy the Gallavotti-Cohen relation, partial ones do not. If the same phenomena occurs for local entropy production then the possibility of the fluctuation relation being observed in a macroscopic system becomes highly dubious. Slow decay of correlations between the partial contraction seems to be responsible for this phenomenon.**

## I. INTRODUCTION

The microscopic structure of systems through which there is transport of energy or momentum is a central problem in nonequilibrium statistical mechanics. For gases a partial answer to this question (on the mesoscopic/kinetic level) is provided by the stationary solution of the Boltzmann equation with suitable, e.g., Maxwellian, boundary conditions. Going beyond kinetic theory has proven to be very difficult and we still lack a full understanding of stationary nonequilibrium states (SNS) on the microscopic level.

This gap goes beyond that of computational complexity or even of technical difficulty in proving the validity of the formulas derived formally, something already present also in the kinetic theory and in equilibrium statistical mechanics. What is still missing, at the present time, are well defined formal procedure which would, at least in principle, provide answers to questions of physical relevance for SNS of macroscopic systems. Thus we have no “statistical mechanical formula” for the decay of spatial or time displaced correlation functions in a SNS. In particular, we have no *a priori* formalism for deciding on the slow power law decay of the

spatial correlations predicted by computer simulations, fluctuating hydrodynamics and confirmed by experiments.<sup>1</sup> We also have no formula for computing the stationary heat flux through a metal or plasma or the momentum flux through a fluid which goes beyond linear response theory. Such a formula should, like the Green-Kubo formula for linear transport, depend only on the internal Hamiltonian of the system and the impressed macroscopic constraints driving the system, e.g., a specified temperature or velocity field on the boundaries of the system.

While the usual modeling of such systems has been via stochastic boundaries<sup>2</sup> there has been much interest recently in the study of SNS of particle systems evolving via entirely deterministic dynamics in the hope that dynamical systems theory will provide new insights into nonequilibrium behavior.<sup>3,4</sup> As is well known the existence of such SNS in finite systems is incompatible with the usual Hamiltonian evolution, believed to accurately describe the dynamics of systems in which quantum effects are unimportant. For such dynamics the only realizable stationary states are those which depend solely on the global constants of motion. In realistic systems these are just the total energy and (under suitable boundary conditions) the total momentum and angular momentum.

Adding external (globally nongradient) forces to the dynamics, e.g., a uniform field in a system with periodic boundary conditions (such as would arise from a changing magnetic flux crossing the surface bounded by a conductor), will typically result in the system gaining energy continuously from the field, excluding the possibility of SNS. This necessitates the use of non phase space volume conserving forces for modeling SNS. Various models of such dynamics have been investigated through computer simulations and heuristic analysis,<sup>4</sup> and there have also been some math-

<sup>a)</sup>Electronic mail: bonetto@hilbert.rutgers.edu

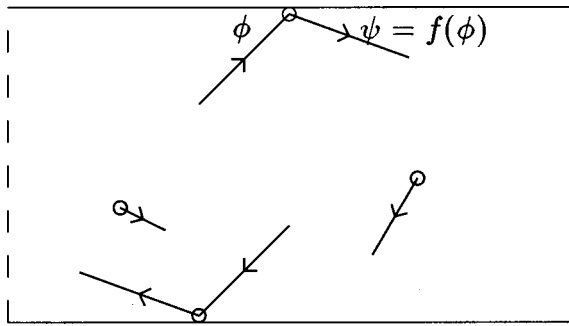


FIG. 1. Schematic representation of the dynamics of the system.

ematical results motivated by physical considerations of such SNS.<sup>5</sup> There is, however, as already mentioned, still a very wide gap between the mathematical and physical results obtained from these models and a full theory of macroscopic SNS.

While it is not clear at present whether and how the dynamical system approach will answer such questions it seems reasonable to explore the behavior of such SNS. This is particularly so for models in which the imposed, model dependent, driving and thermostating terms are confined to the boundaries of the system while the dynamics in the interior of the system remain realistically Hamiltonian. Several such models of shear flow were investigated via computer simulations and some heuristic analysis in Ref. 6. Here we continue our investigation focusing on the behavior of the fluctuation in the phase space volume contraction  $\sigma$  which occurs at the boundaries.  $\sigma$  was found in Ref. 6 to be approximately equal, when the size of the system is sufficiently large for it to be in local thermal equilibrium, to the hydrodynamic entropy production inside the system. The same quantity, in a different model of shear flow, was studied in Ref. 7 where an interesting relation for its large deviations was experimentally found. This relation is now a rigorous result for large deviations of phase space contraction under suitable conditions on the dynamics.<sup>5</sup> Whether the results hold when the conditions are not satisfied exactly is a question of great relevance. The exploration of this and related quantities is the subject of the present work.

In the next section we describe the model and the check of the Gallavotti-Cohen result<sup>5</sup> for our system. In Sec. III we investigate fluctuations and time dependent correlations of the volume contractions  $\sigma^\uparrow$  and  $\sigma^\downarrow$  produced by collisions with the top and bottom walls.

## II. NUMERICAL SIMULATIONS: THE FLUCTUATION THEOREM

### A. The model

We consider the two-dimensional shear flow model first introduced in Ref. 6 and further studied in Ref. 8:  $N$  identical disks of radius  $r$  evolve in the interior of the system according to Hamiltonian dynamics with hard core interaction among them while Maxwell demons at the walls drive the system away from equilibrium. More specifically the particles move on the surface of a cylinder (i.e., the system has periodic boundary conditions on the vertical sides) with re-

TABLE I. Static and dynamic quantity for the simulation.

	10	20	30	40
$d$	$3.4 \times 10^{-2}$	$3.4 \times 10^{-2}$	$3.4 \times 10^{-2}$	
$t_0$	20.6	30.6	38.1	44.4
$\nu$	2.11	3.19	4.00	4.67
$\langle \alpha \rangle_+$	$1.24 \times 10^{-2}$	$1.68 \times 10^{-2}$	$2.00 \times 10^{-2}$	$2.26 \times 10^{-2}$
$\lambda_{\max}$	0.92	0.74	0.63	0.57

flection rules at the top and bottom walls simulating macroscopic moving walls. The rules are as follows: when a particle collides with the upper wall, making an angle  $\phi$  between the positive  $x$ -direction and the incoming velocity then the outgoing velocity angle  $\psi$  will be given by a (to be specified) reflection rule  $f$ :

$$\psi = f(\phi). \quad (2.1)$$

A similar rule applies on the lower wall with the only difference that  $\psi$  and  $\phi$  refer to the angle between the incoming and outgoing velocity and the negative  $x$ -direction. Since the modulus of the velocity is preserved during a collision the total kinetic energy of the system is a constant of the motion.

We will assume that  $f$  is “time reversible,” i.e., it satisfies  $\phi = f(\pi - f(\pi - \phi))$ . Observe that if this condition holds the system is time reversible: if one inverts the velocities of all the particles the system traces back its past trajectory. In the numerical simulations we will consider one of the reflection rules introduced in Ref. 6, namely,

$$\psi = (\pi + b) - \sqrt{(\pi + b)^2 - \phi(\phi + 2b)}, \quad (2.2)$$

where  $b$  is used to modulate the intensity of the shear with  $b = \infty$  representing elastic collisions (see Fig. 1).

During a collision with the walls the Liouville measure is not conserved. In fact at each “reflection” there is a phase space contraction  $\alpha$  equal to<sup>6</sup>

$$\alpha = -\log \left( \frac{\sin \psi}{\sin \phi} f'(\phi) \right). \quad (2.3)$$

It is natural to consider the collisions with the walls as timing events for the system. This is, we can consider the function  $T$  that associates to any point  $X$  in the phase space of the system, i.e., the energy surface  $\Sigma$ , the first time at which a particle collides with a wall and define the map,  $S: \Sigma \rightarrow \tilde{\Sigma}$ ,  $S(X) = F(\Phi(X, T(X)))$ , where  $\tilde{\Sigma}$  is the set of points at which at least one particle is colliding with the walls,  $\Phi(X, t)$  is the point  $X_t$  obtained from  $X$  via the flow generated by the dynamics, and  $F: \tilde{\Sigma} \rightarrow \tilde{\Sigma}$  is the collision map, i.e., the map that changes the velocity of the colliding particle according to the reflection rule  $f$ .

Given a point  $X$  we define

$$\alpha_\tau(X) = \sum_{i=-[\tau/2]}^{[\tau/2]-1} \alpha(S^i(X)) \quad (2.4)$$

and

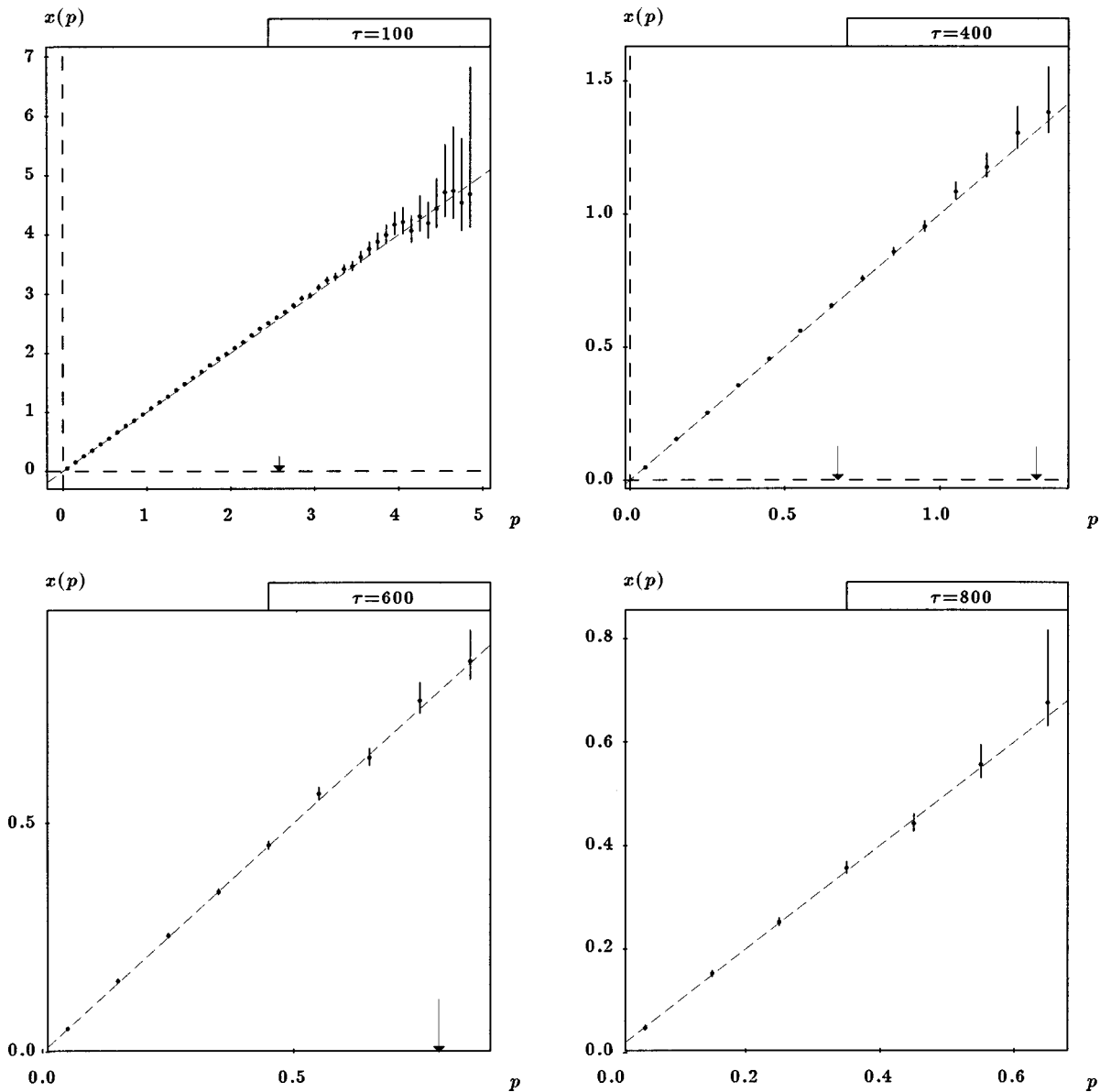


FIG. 2. Graphs of  $x_\tau(p)$  for  $\tau=100, 400, 600,$  and  $800$  for  $N=20$ . The arrows represents the value 1 plus or minus the standard deviation of  $\sigma_\tau$ .

$$\sigma_\tau(X) = \frac{\alpha_\tau(X)}{\langle \alpha_\tau \rangle_+}, \tag{2.5}$$

where  $[t]$  is the biggest integer less than  $t$ ,  $\langle \cdot \rangle_+$  refer to the mean with respect to the forward invariant distribution. Call  $\pi_\tau(p)$  the distribution function of  $\sigma_\tau$ , and let

$$x_\tau(p) = \frac{1}{\langle \alpha_\tau \rangle_+} \log \frac{\pi_\tau(p)}{\pi_\tau(-p)} \tag{2.6}$$

then the chaotic hypothesis of Ref. 5 implies that

$$\lim_{\tau \rightarrow \infty} x_\tau(p) = p. \tag{2.7}$$

To check numerically this relation simulations were carried out on systems of  $N=10, 20, 30$  and  $40$  particles of radius  $R=1$  in a “square” box of size  $L=\sqrt{dN}$ , where  $d=N/L^2$  is the number density kept constant to  $d=3.4 \times 10^{-2}$ , and with the parameter  $b=25$ . The initial configuration was chosen randomly in such a way that the energy

per particle  $e_0=(1/2N)\sum_{i=0}^N v_i^2=0.5$ . In Table I we give some of the interesting dynamical quantities associated with the system.

Here  $t_0$  is the mean time between successive collisions with the walls for a given particle,  $\nu$  is the number of binary collisions (i.e., collisions between two particles) between two consecutive collisions with the walls for a given particle and  $\langle \alpha \rangle_+$  is the mean phase space contraction rate. Finally we give the maximum Lyapunov exponent of the map  $S$ . The data, given without error estimates, are intended to give a rough image of the dynamics.

### B. The fluctuation law

The check of the fluctuation theorem was done as in Ref. 9. A long trajectory of  $5 \times 10^8$  collisions with the walls was simulated and the phase space contraction was recorded for every 100 collisions. The main difference with Ref. 9 is that we did not attempt to decorrelate the adjacent data segment

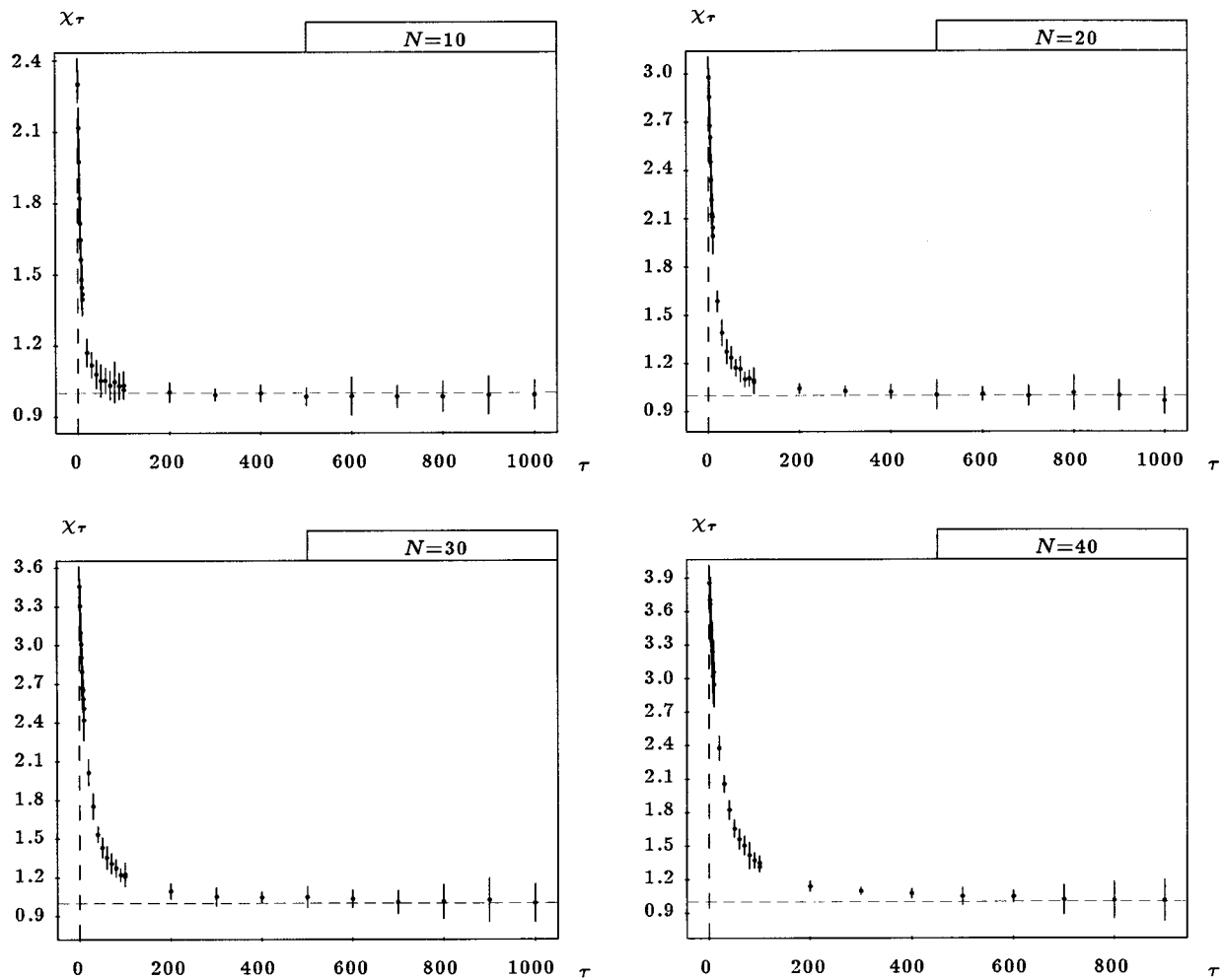


FIG. 3. Behavior of  $\chi_\tau$  as a function of  $\tau$  for  $N=10, 20, 30,$  and  $40$ .

by leaving out a fixed number of collisions between them. In fact in Ref. 9 this was possible because the self-correlation of the phase space contraction was decaying rapidly enough to leave out just a few collisions. In the present system we find that while the total phase space contraction rate has rapidly decaying correlation the partial ones (to be defined precisely and studied in the next section) have a very slow decay. Hence we would have to discard too many collisions to decorrelate the adjacent data segments, and we therefore decided to discard no collisions also for the total phase space contraction to have a consistent analysis.

In Fig. 2 we show the graph of  $x_\tau(p)$  for  $N=20$  and several values of  $\tau$ . As we can see already for  $\tau=400$  the agreement between the theoretical prediction and the experiment is very good.

To better follow the behavior of the fluctuation we have constructed the function  $x_\tau(p)$  for  $N=10, 20, 30$  and  $40$  for several values of  $\tau$  from 1 to 1000. We have then used a least-squares-fit to fit the experimental data with a law of the form  $x_\tau(p) = \chi_\tau p$ . We chose a one parameter fit because  $x_\tau(0) \equiv 0$ . The results are shown in Fig. 3. As can be easily seen the evaluated  $\chi_\tau$  contain 1 within their error-bars starting from a quite small value of  $\tau$ . Moreover, one appears to be the asymptotical value of  $\chi_\tau$ .

The analysis of the fluctuation law requires the construction of the whole distribution function  $\pi_\tau(p)$ . But as  $\tau$  grows big fluctuations become more and more improbable and it is impossible to construct  $x_\tau(p)$  for  $\tau > 1000$ . To go further with  $\tau$  we can observe that, starting with  $\tau \approx 5$ , the distribution  $\pi_\tau(p)$  look very much like a Gaussian. Observe that if we assume that the system is Anosov the central limit theorem implies a Gaussian behavior near the maximum of the distribution but the observed agreement goes, in our opinion, beyond the prediction of the central limit theorem. Nevertheless it must be noted that the distribution cannot be Gaussian because it is easy to observe that  $|\alpha_\tau(X)|$  is bounded. Figure 4 shows the comparison with a Gaussian for  $N=20$  and several values of  $\tau$ .

Assuming that  $\pi_\tau$  is a Gaussian immediately implies that  $x_\tau(p)$  is linear in  $p$  and, calling  $C_\tau$  the covariance of  $\sigma_\tau$ , i.e.,  $C_\tau = \langle \sigma_\tau^2 \rangle - 1$ , we have that

$$\chi_\tau = \frac{2}{\langle \alpha_\tau \rangle C_\tau}. \quad (2.8)$$

The covariance  $C_\tau$  can be easily computed from the data and permits us to go beyond the limit of  $\tau=100$  met before.

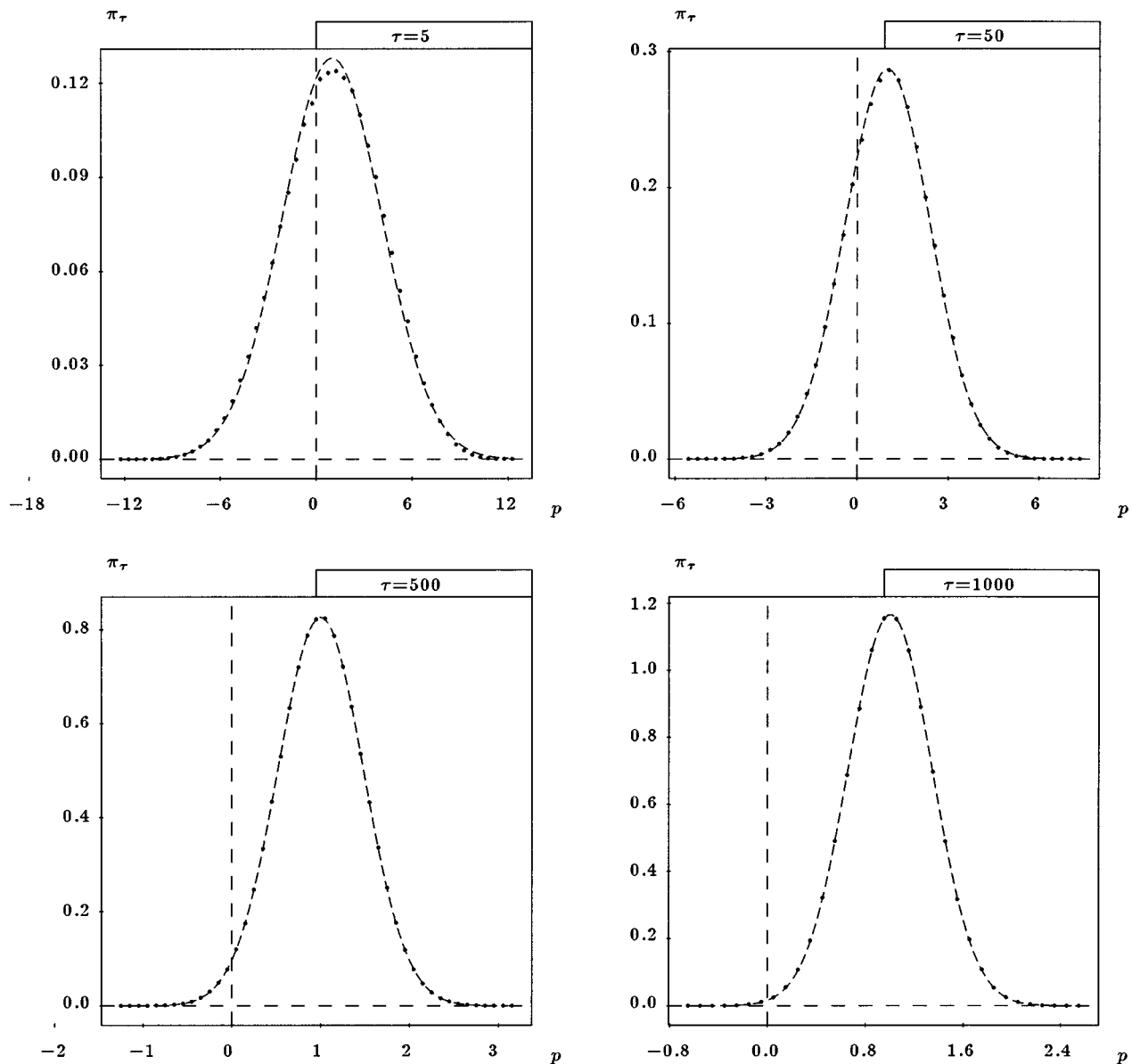


FIG. 4. Comparison between the distribution  $\pi_\tau(p)$  for  $N=20$  and several values of  $\tau$ , and a Gaussian with the same variance and mean. The error-bars are smaller than the dimension of the points.

As a further check we show the value of  $\chi_\tau$  as computed from the best fit and from the Gaussian hypothesis for a small value of  $\tau$  in Fig. 5.

The agreement is very good and justifies the use of Eq. (2.8) for large value of  $\tau$ . The evaluated behavior of  $\chi_\tau$  for a large value of  $\tau$  from the Gaussian hypothesis is shown in Fig. 6.

In all cases the values of  $\chi_\tau$  are very close to 1 and we can therefore say that the prediction of the fluctuation law appears to be verified by our numerical simulations.

Finally observe that the approach to 1 of  $\chi_\tau$  can be connected to the decay property of the autocorrelation  $D(t) = \langle \sigma(S^t(\cdot))\sigma(\cdot) \rangle - 1$ . In fact we have

$$C(\tau) = \frac{2}{\tau} \sum_{t=-\tau}^{\tau} D(t) - \frac{2}{\tau^2} \sum_{t=-\tau}^{\tau} |t| D(t). \tag{2.9}$$

The fast approach of  $\chi_\tau$  to its limit can thus be inter-

preted as a rapid decay of the correlation for the phase space contraction of the system. We will see that this behavior changes greatly when we consider partial phase space contractions.

### III. LOCAL FLUCTUATIONS

An interesting question is whether one can give a local version of the fluctuation theorem. To this extent observe that we can write  $\alpha_\tau(X) = \alpha_\tau^\uparrow(X) + \alpha_\tau^\downarrow(X)$  where

$$\alpha_\tau^\uparrow(X) = \sum_{i=-[\tau/2]}^{[\tau/2]} \alpha(S^i(X)) \chi^\uparrow(S^i(X)) \tag{3.1}$$

and  $\chi^\uparrow(x) = 1$  if  $X$  corresponds to a collision of a particle with the upper wall and 0 otherwise. An analogous definition holds for  $\alpha_\tau^\downarrow(X)$ .

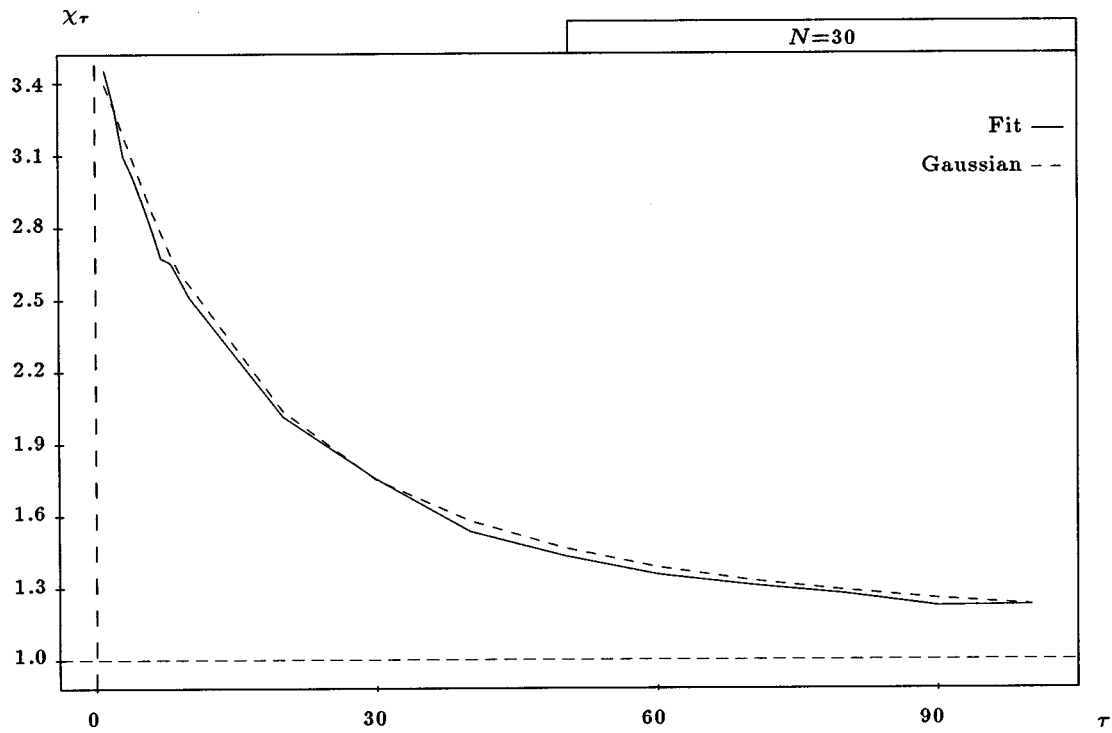


FIG. 5. Comparison between the value of  $\chi_\tau$  computed directly and using the Gaussian hypothesis for  $N=30$ . Similar results are found for  $N=10, 20$ , and  $40$ .

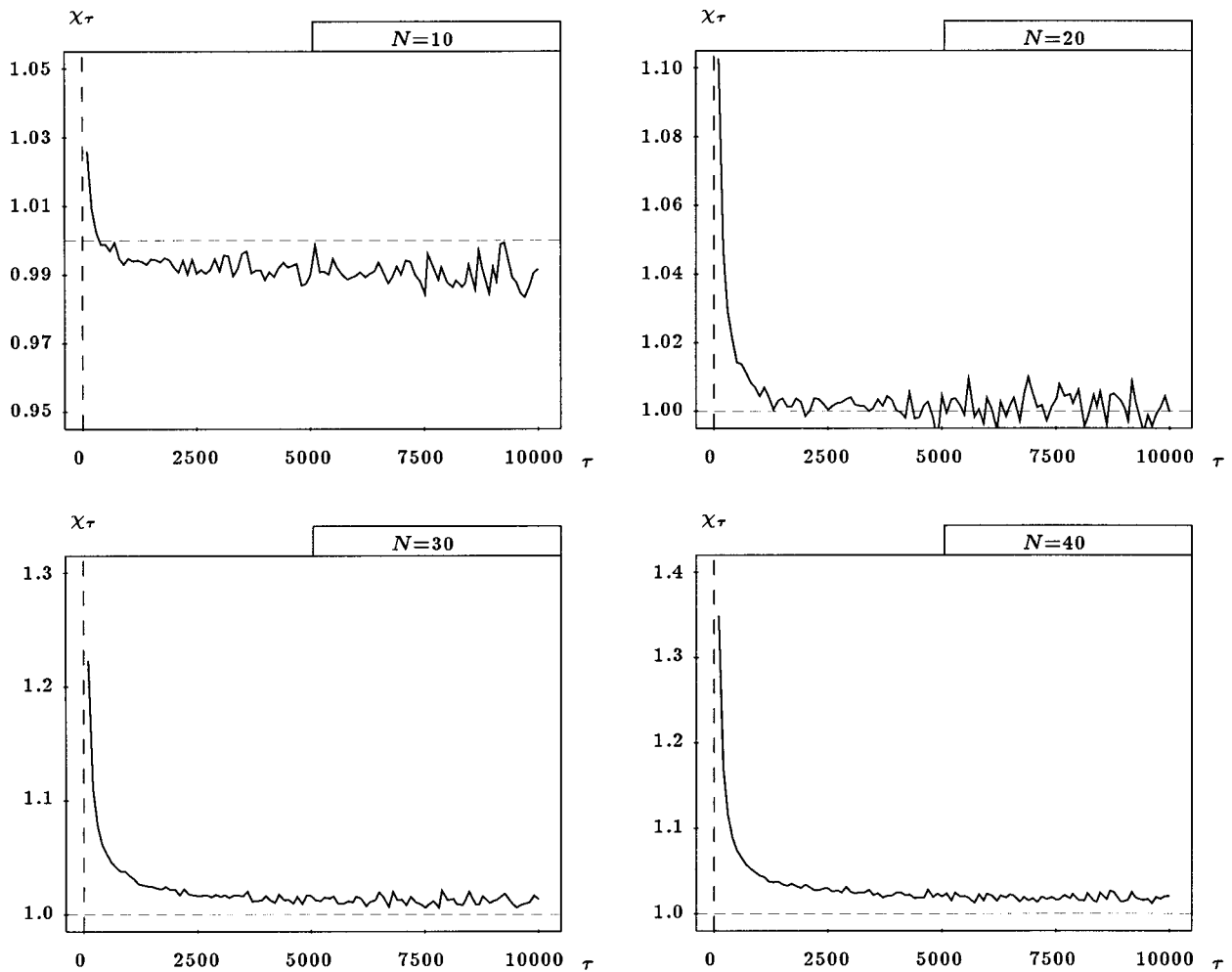


FIG. 6. Value of  $\chi_\tau$  obtained from the Gaussian hypothesis for large  $\tau$ .

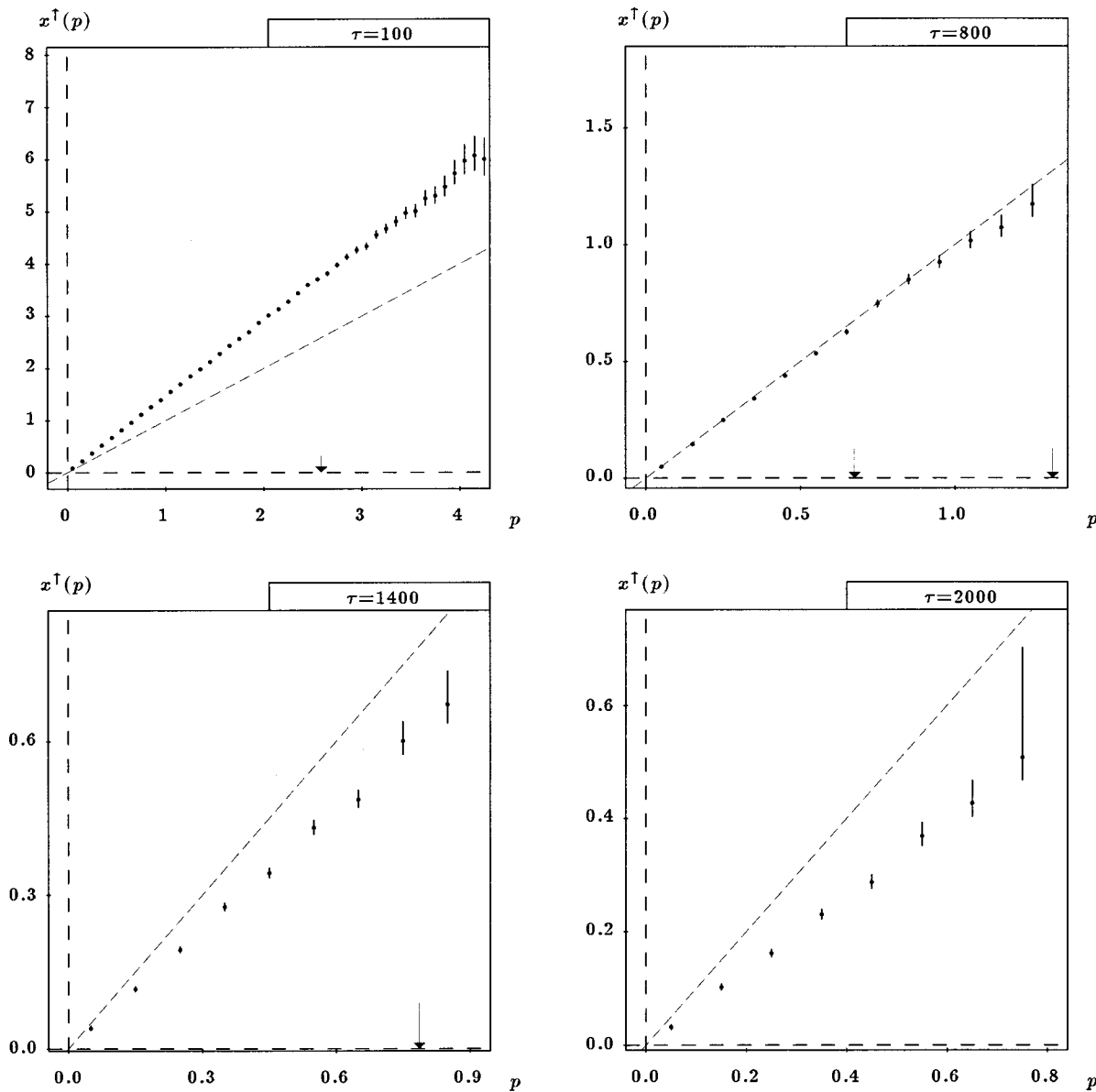


FIG. 7. Graphs of  $x_\tau^\uparrow(p)$  for  $\tau=100, 800, 1400$ , and  $2000$  for  $N=20$ . The arrows represents the value 1 plus or minus the standard deviation of  $\sigma_\tau^\uparrow$ .

The generalized version of the fluctuation theorem of Ref. 10 gives

$$\lim_{\tau \rightarrow \infty} \frac{1}{\langle \alpha_\tau^\uparrow \rangle_+} \log \frac{\pi_\tau^{\uparrow\downarrow}(p_1, p_2)}{\pi_\tau^{\uparrow\downarrow}(-p_1, -p_2)} = p_1 + p_2, \tag{3.2}$$

where  $\pi_\tau^{\uparrow\downarrow}(p_1, p_2)$  is the joint distribution of  $\sigma_\tau^\uparrow(X) = \alpha_\tau^\uparrow(X) / \langle \alpha_\tau^\uparrow \rangle_+$  and  $\sigma_\tau^\downarrow(X) = \alpha_\tau^\downarrow(X) / \langle \alpha_\tau^\downarrow \rangle_+$ . Due to the symmetry of the problem the two variables  $\sigma_\tau^\uparrow(X)$  and  $\sigma_\tau^\downarrow(X)$  can be assumed to be identically distributed. (Although this is well verified numerically it is not evident from a theoretical point of view. It is in fact easy to see that if the particles do not interact, i.e., they do not collide, the mean momentum of the center of mass is, generically, not zero and this will probably create asymmetry between the two walls. This phenomenon is probably destroyed by the ‘‘mixing’’ behavior generated by the binary collisions. It must be nevertheless noted that for small systems, like ours, the fluctuations of the center of mass momentum are quite big and its correlations

decay slowly.) It is easy to see that if we suppose them independent, both of them will separately satisfy the fluctuation theorem:

$$\lim_{\tau \rightarrow \infty} x_\tau^\uparrow(p) = p, \tag{3.3}$$

where

$$x_\tau^\uparrow(p) = \frac{1}{\langle \alpha_\tau^\uparrow \rangle_+} \log \frac{\pi_\tau^\uparrow(p)}{\pi_\tau^\uparrow(-p)}. \tag{3.4}$$

This can be checked as we did for  $\alpha_\tau(x)$ . In Fig. 7 we show the graph of  $x_\tau^\uparrow(p)$  for  $N=20$  and several values of  $\tau$ .

Observe that here we are able to construct the distribution function  $\pi_\tau$  up to  $\tau=2000$ . This is not surprising considering that  $\alpha_\tau^\uparrow(X)$  is, in the mean, the sum of  $\tau/2$  nonzero terms so that it can be expected to have fluctuations roughly similar to those of  $\alpha_{\tau/2}(X)$ .

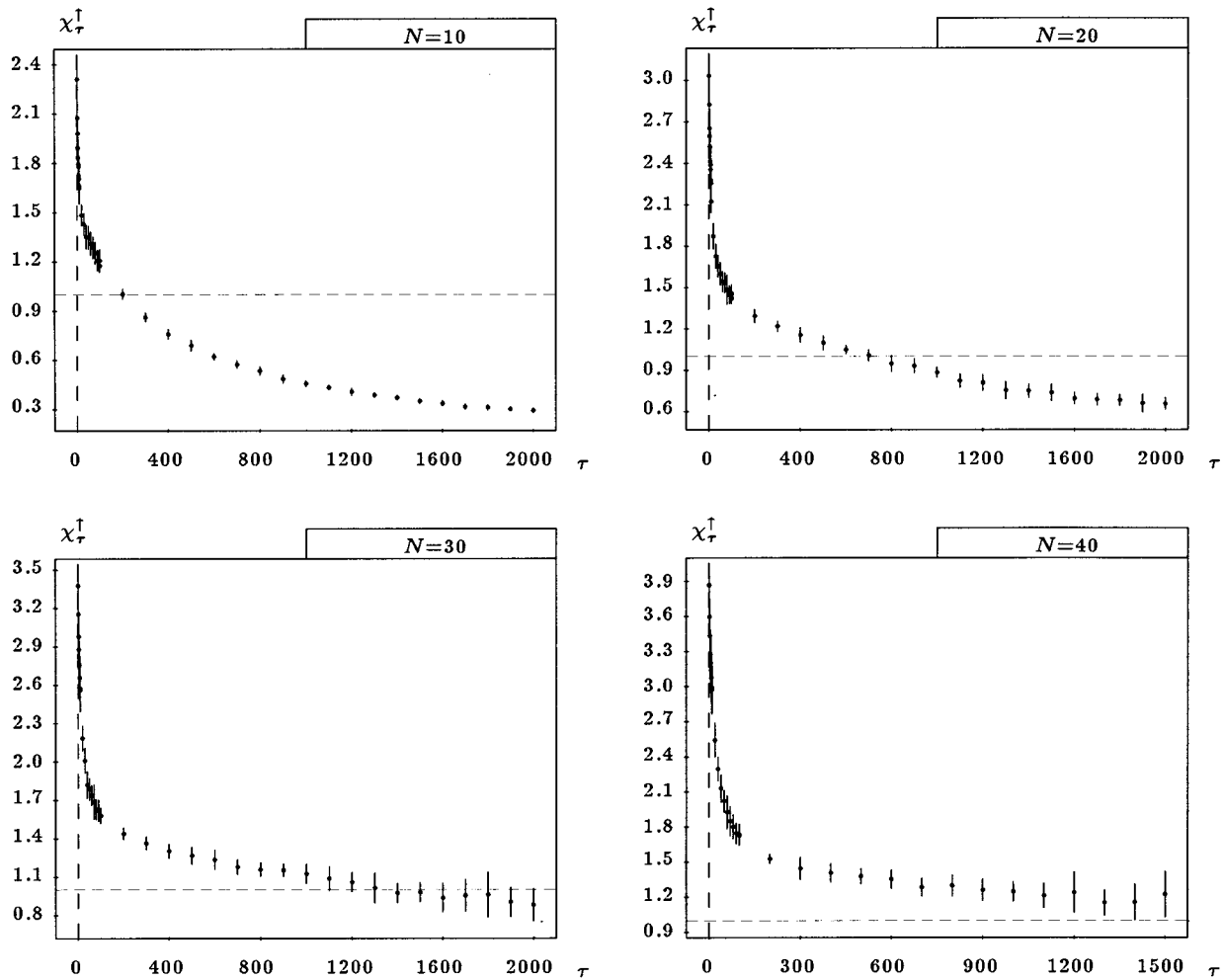


FIG. 8. Behavior of  $\chi_\tau^\uparrow$  as a function of  $\tau$  for  $N=10, 20, 30,$  and  $40$ .

As before we can look at the best fit of  $x_\tau^\uparrow(p)$  of the form  $x_\tau^\uparrow(p) = \chi_\tau^\uparrow p$ . The results are shown in Fig. 8.

It is clear that for  $N=10$  and  $20$  the fit goes significantly below 1 at a value of  $\tau$  for which  $\chi_\tau$  is very near its theoretical value of 1. Moreover  $\chi_\tau^\uparrow$  does not seem to have reached a limiting value while  $\chi_\tau$  reaches its limiting value of 1 quite soon.

The cases  $N=30$  and  $40$  are less clear because we are unable to construct the distribution function for  $\tau$  large enough to have a clear idea of the limiting value of  $\chi_\tau$ . But it seems reasonable to deduce from the graph that also in this case  $\chi_\tau$  will become smaller than 1.

Considering the argument at the beginning of this section it is interesting to look at the cross correlation between  $\sigma_\tau^\uparrow$  and  $\sigma_\tau^\downarrow$  given by

$$C_\tau^{\uparrow\downarrow} = \langle \sigma_\tau^\uparrow \sigma_\tau^\downarrow \rangle_+ - 1$$

whose graph is plotted in Fig. 9.

It is interesting to note that, if we disregard the value of  $C_\tau^{\uparrow\downarrow}$  for a small value of  $\tau$ , we have that the behavior of  $C_\tau^{\uparrow\downarrow}$  is linked to that of  $\chi_\tau$ . In particular we can see that when  $C_\tau^{\uparrow\downarrow} = 0$  we have  $\chi_\tau = 1$ . This is particularly clear in the cases  $N=10$  and  $20$ .

This suggests that the higher order correlations of  $\sigma^\uparrow$  and  $\sigma^\downarrow$  are small compared to the second order correlation. Moreover the distribution function  $\pi_\tau^\uparrow$  is again very well approximated by a Gaussian as can be seen in Fig. 10.

As in the previous section we can assume that the pair  $(\sigma^\uparrow, \sigma^\downarrow)$  represents a bidimensional Gaussian variable with mean  $(1,1)$  and covariance matrix:

$$C_\tau = \begin{pmatrix} C_\tau^\uparrow & C_\tau^{\uparrow\downarrow} \\ C_\tau^{\uparrow\downarrow} & C_\tau^\downarrow \end{pmatrix}, \tag{3.5}$$

where

$$C_\tau^\uparrow = \langle (\sigma_\tau^\uparrow)^2 \rangle - 1, \quad C_\tau^\downarrow = \langle (\sigma_\tau^\downarrow)^2 \rangle - 1. \tag{3.6}$$

From now on we will suppose that  $C_\tau^\uparrow = C_\tau^\downarrow$ . This is well verified in the experiment and seems natural from the symmetry properties of the system. (See, however, the comment at the beginning of Sec. II B.) With the above Gaussian hypothesis we can again try to follow the behavior of  $\chi_\tau^\uparrow$  for a large value of  $\tau$  using the expression

$$\chi_\tau^\uparrow = \frac{2}{\langle \alpha^\uparrow \rangle \tau C_\tau^{\uparrow\downarrow}}. \tag{3.7}$$



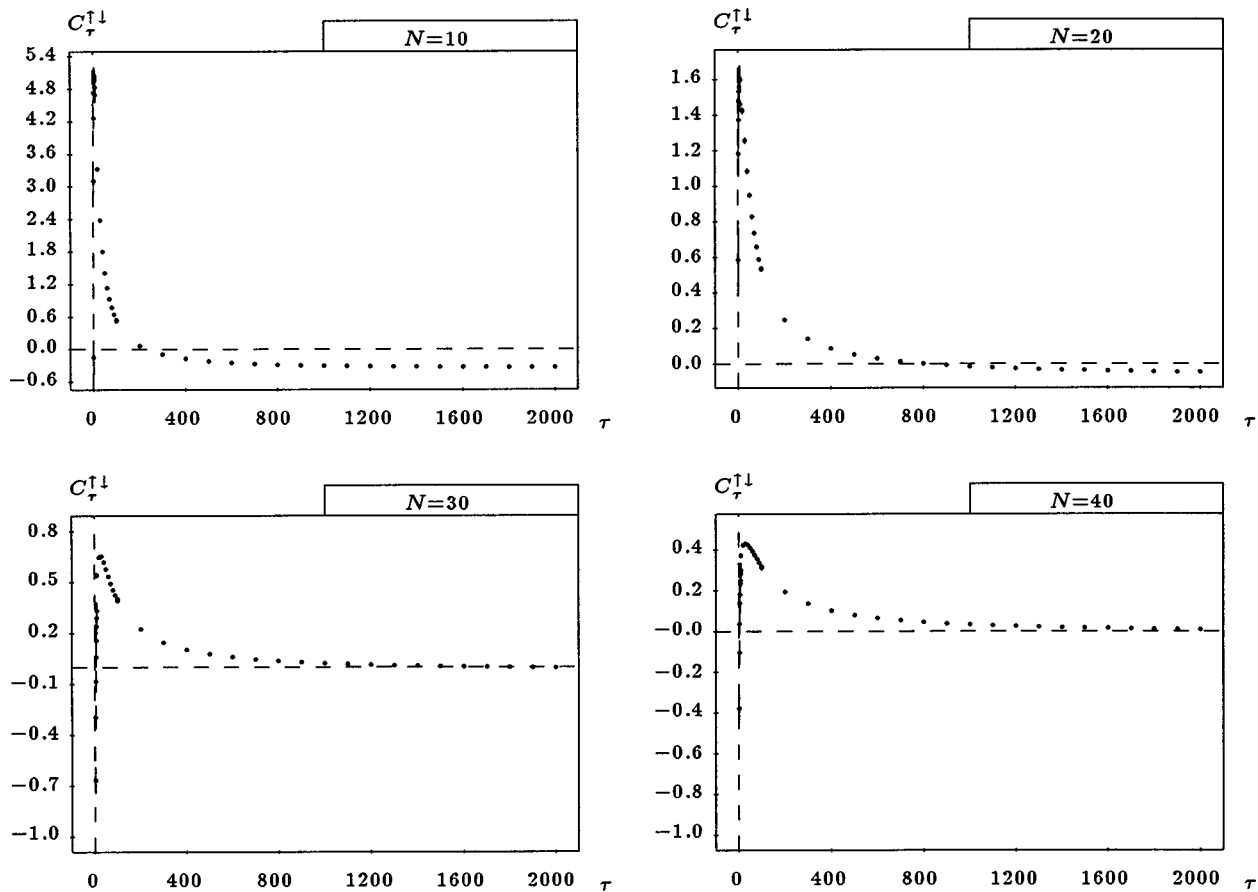


FIG. 9. Behavior of  $C_\tau^{\uparrow\downarrow}$  as a function of  $\tau$  for  $N=10, 20, 30,$  and  $40$ .

Figure 11 shows the results of this evaluation.

Finally we observe that we can write

$$C_\tau^{\uparrow\downarrow} = 2C_\tau - C_\tau^{\uparrow}. \tag{3.8}$$

Hence if we assume Gaussianity and take  $\tau$  large enough that we can consider  $\chi_\tau = 1$ , this gives

$$K_\tau = \chi_\tau^{\uparrow} - 1 = \frac{C_\tau^{\uparrow\downarrow}}{C_\tau^{\uparrow}}. \tag{3.9}$$

We can conclude this discussion by observing that, for finite  $N$ , the fluctuation law seems to be invalid if we take into consideration only half of the entropy production. Nevertheless it is interesting to note that  $x_\tau^{\uparrow\downarrow}(p)$  still look linear and that the slope  $\chi_\tau^{\uparrow\downarrow}$  seems to reach a finite limit as  $\tau$  goes to infinity. Moreover this limit is very small for small  $N$  and seems to increase with  $N$ . It would be interesting to fit the curve in Fig. 11 to give an estimate of the limiting value of  $\chi_\tau^{\uparrow}$  as  $\tau \rightarrow \infty$ . We observe that, as for  $\chi_\tau$ , we can relate the approach to a limiting value of  $\chi_\tau^{\uparrow}$  with the decay properties of  $D^\uparrow(t) = \langle \sigma^\uparrow(S^t(\cdot)) \sigma^\uparrow(\cdot) \rangle - 1$ . In fact an equation identical to (2.9) holds for  $C_\tau^{\uparrow}$  with  $D^\uparrow(t)$  in the place of  $D(t)$ . A comparison of Figs. 6 and 11 immediately shows that the decay of correlations of  $\sigma^\uparrow$  is much slower that of  $\sigma$ . If we assume that  $D^\uparrow(t) \approx t^{-\beta}$ , with  $\beta > 0$ , we get that:

$$\chi_\tau^{\uparrow} = \chi_\infty^{\uparrow} + \frac{\chi^{\uparrow\prime}}{\tau} + \frac{\chi^{\uparrow\prime\prime}}{\tau^{\beta-1}}.$$

If  $\beta$  is smaller than 2 the third term dominates in the asymptotic behavior on the second one. One can try to fit  $\beta$  looking at the log-log plot of  $\chi_\tau^{\uparrow}$  and then using a least-squares fit to find the other coefficient. Unfortunately the log-log plot does not give a precise answer, so we can only say that  $\beta$  is probably less than 2. This implies that the approach to the limit of  $\chi_\tau^{\uparrow\downarrow}$  is very slow and its limiting value changes considerably depending which  $\beta$  one uses. At the end we are unable to give a quantitative estimate of  $\chi_\infty^{\uparrow\downarrow}$  and we can just say that it is nonzero and increases with  $N$ .

#### IV. CONCLUSION

Our numerical results show that the fluctuation theorem, Eq. (2.5), is well verified if we consider the total phase space contraction  $\sigma$  of the model described in Sec. I A. For  $\tau$  small enough we were able to construct the distribution  $\pi_\tau(p)$  and check directly the validity of Eq. (2.5). For higher  $\tau$  we used a Gaussian hypothesis to compute the slope  $\chi_\tau$  of  $x_\tau(p)$  obtaining again a very good agreement with the theoretical prediction. We observe that if we interpret the Gaussianity of  $\pi_\tau(p)$  as a central limit theorem effect we get that  $x_\tau(p)$  is linear but no conclusion can be drawn on the slope  $\chi_\tau$ . The validity of the fluctuation theorem predictions, together with the Gaussian hypothesis, imply a Green-Kubo formula out of equilibrium as can be seen by combining Eqs. (2.8) and (2.9) (see also Ref. 9). In this sense we can think that our results depend in part on the fact that we are not very far from

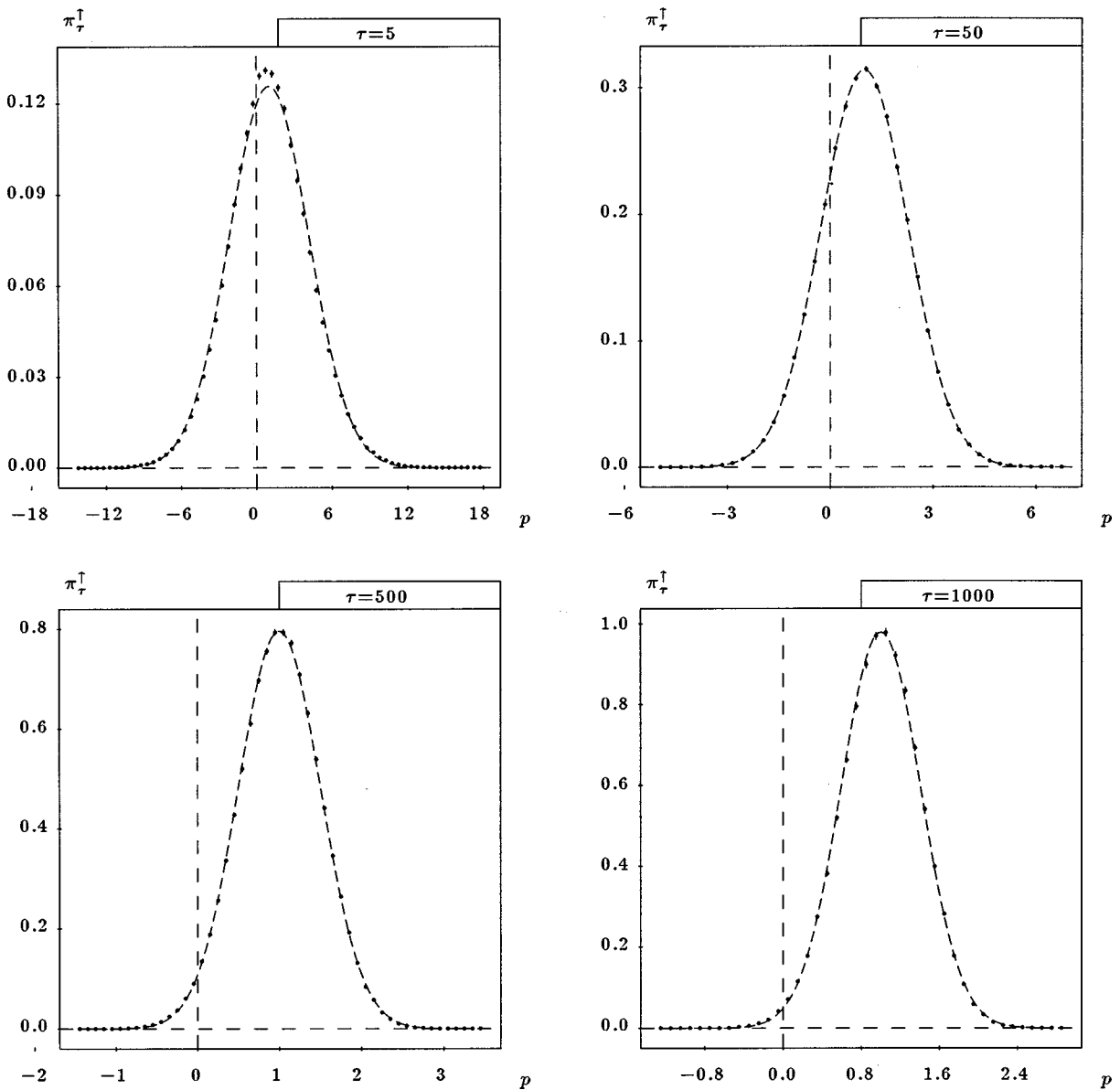


FIG. 10. Comparison between the distribution  $\pi_\tau^\uparrow(p)$  and a Gaussian with the same variance and mean. The errorbars are smaller than the dimension of the points.

equilibrium. Increasing the shear makes the experiment much harder because the probability of observing negative fluctuations decreases very rapidly with the shear. Moreover we expect that the Gaussianity of  $\pi_\tau(p)$  will be destroyed. We think, however, that if the shear is not too big, i.e., if the attractor can still be considered dense in phase space (see Ref. 11), then the fluctuation theorem will hold [see Ref. 12 for a situation in which  $\pi_\tau(p)$  is clearly not Gaussian].

We also checked the validity of the fluctuation theorem for the partial phase space contraction  $\sigma^\uparrow$  and  $\sigma^\downarrow$ . In this situation we see that  $\pi_\tau^{\uparrow,\downarrow}$  is still well approximated by a Gaussian so that  $x_\tau^{\uparrow,\downarrow}(p)$  appears to be linear. The slope  $\chi_\tau^{\uparrow,\downarrow}$ , however, behaves in a different way from what one would expect. Two interesting features of this behavior are

(1) It saturates very slowly. The fact that we considered, in the definition of  $\sigma_\tau^{\uparrow,\downarrow}$ , a fixed number of collisions  $\tau$  with both walls clearly creates a negative correlation between  $\sigma_\tau^\uparrow$

and  $\sigma_\tau^\downarrow$ . This correlation can be roughly estimated as  $\tau^{-1}$  so that it probably cannot account for the slow behavior found in Sec. III. That behavior shows a strong correlation between the two walls probably due to the slow decay of fluctuation of the density near the walls. We do not have a clear understanding of this phenomenon and we hope to come back on it in a forthcoming work.

(2) The limiting value  $\chi_\infty^{\uparrow,\downarrow}$  is not easy to estimate but is clearly smaller than 1. Although it seems to increase with the number of particles we do not have enough data to draw any conclusion on its behavior with  $N$ . Nevertheless the existence of a limiting nonzero value suggests the validity of a ‘‘local fluctuation theorem’’ in which the slope 1 is replaced by some other value. This behavior may have relations to the recent experimental result on the local entropy production (supposed to be the equivalent of a phase space contraction) in a fluid moving in a convective cell.<sup>13</sup> They find there a

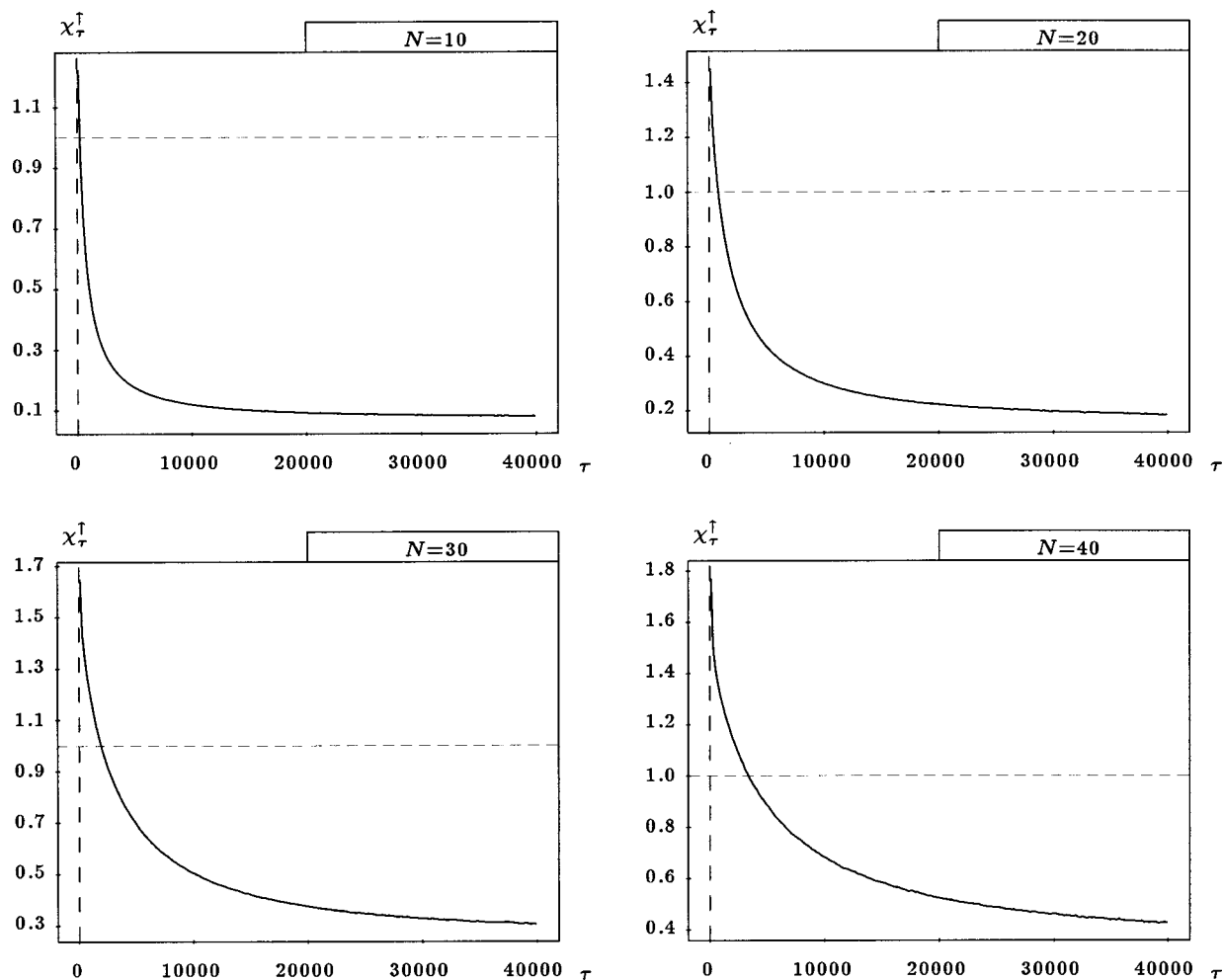


FIG. 11. Behavior of  $\chi_\tau^\dagger$  as a function of  $\tau$  for  $N=10, 20, 30,$  and  $40$ .

clear linear behavior but the slope seems to be different from one. The results are, however, still unclear and no real comparison can be made.

**ACKNOWLEDGMENTS**

F.B. is indebted to E.G.D. Cohen and G. Gallavotti for many helpful discussions and suggestions. N.I.C. was partly supported by NFS Grant No. DMS-9654622. F.B. and J.L.L. were in part supported by NFS Grant No. DMR-9523266.

<sup>1</sup>Z. Cheng, P. L. Garrido, and J. L. Lebowitz, "Correlations in stationary nonequilibrium systems with conservative anisotropic dynamics," *Europhys. Lett.* **14**, 507–513 (1991).  
<sup>2</sup>G. Eyink, J. L. Lebowitz, and H. Spohn, "Lattice gas model in contact with stochastic reservoirs: Local equilibrium and relaxation to steady states," *Commun. Math. Phys.* **140**, 119–132 (1991).  
<sup>3</sup>G. Gallavotti, "New methods in nonequilibrium gases and fluids," archived in mp-arc at [www.ma.utexas.edu](http://www.ma.utexas.edu) #96-533; D. Ruelle, "Dynamical Systems Approach to Nonequilibrium Statistical Mechanics: An Introduction," IHES/Rutgers, Lecture Notes, 1997.

<sup>4</sup>D. J. Evans and G. P. Morris, *Statistical Mechanics of Nonequilibrium Liquids* (Academic, New York, 1990).  
<sup>5</sup>G. Gallavotti and E. G. D. Cohen, "Dynamical ensemble in a stationary state," *J. Stat. Phys.* **80**, 931–970 (1995).  
<sup>6</sup>N. I. Chernov and J. L. Lebowitz, "Stationary nonequilibrium states for boundary driven Hamiltonian systems," *J. Stat. Phys.* **86**, 953–990 (1997).  
<sup>7</sup>D. J. Evans, E. G. D. Cohen, and G. P. Morris, "Probability of second law violations in shearing steady flows," *Phys. Rev. Lett.* **71**, 2401–2404 (1993).  
<sup>8</sup>C. Dellago and H. A. Posch, "Lyapunov instability of the boundary driven Chernov-Lebowitz model for stationary shear flow," *J. Stat. Phys.* **88**, 825–842 (1997).  
<sup>9</sup>F. Bonetto, G. Gallavotti, and P. L. Garrido, "Chaotic principle: an experimental test," *Physica D* **105**, 226–252 (1997).  
<sup>10</sup>G. Gallavotti, "Extension of the Onsager reciprocity to large field and the chaotic hypothesis," *Phys. Rev. Lett.* **77**, 4334–4337 (1996).  
<sup>11</sup>F. Bonetto and G. Gallavotti, "Chaotic principle, reversibility and coarse graining," *Commun. Math. Phys.* **189**, 263–276 (1997).  
<sup>12</sup>S. Lepri, R. Livi, and A. Politi, "Energy transport in anharmonic lattice close and far from equilibrium," preprint, archived in [xxx.lanl.gov](http://xxx.lanl.gov) cond-mat #9709195.  
<sup>13</sup>S. Ciliberto, "An experimental verification of the Gallavotti-Cohen fluctuation theorem," preprint.